Earth and Planetary Science Letters 421 (2015) 89–97

Contents lists available at ScienceDirect

Earth and Planetary Science Letters

www.elsevier.com/locate/epsl

Modes of continental extension in a crustal wedge

Guangliang Wu [a,b,*], Luc L. Lavier [a,b], Eunseo Choi [c]

[a] Institute for Geophysics, University of Texas at Austin, 10100 Burnet Rd., Austin, TX 78758-4445, United States
[b] Department of Geological Sciences, University of Texas at Austin, 2225 Speedway, Stop C1160, Austin, TX 78712-1692, United States
[c] Center for Earthquake Research and Information, University of Memphis, 3890 Central Ave., Memphis, TN 38152-3060, United States

ARTICLE INFO

Article history:
Received 31 October 2014
Received in revised form 2 April 2015
Accepted 3 April 2015
Available online xxxx
Editor: Y. Ricard

Keywords:
crustal wedge
extension
core complex
detachment fault
ductile shear zone
decoupling

ABSTRACT

We ran numerical experiments of the extension of a crustal wedge as an approximation to extension in an orogenic belt or a continental margin. We study the effects of the strength of the lower crust and of a weak mid-crustal shear zone on the resulting extension styles. A weak mid-crustal shear zone effectively decouples upper crustal extension from lower crustal flow. Without the mid-crustal shear zone, the degree of coupling between the upper and the lower crust increases and extension of the whole crust tends to focus on the thickest part of the wedge. We identify three distinct modes of extension determined by the strength of the lower crust, which are characterized by 1) localized, asymmetric crustal exhumation in a single massif when the lower crust is weak, 2) the formation of rolling-hinge normal faults and the exhumation of lower crust in multiple core complexes with an intermediate strength lower crust, and 3) distributed domino faulting over the weak mid-crustal shear zone when the lower crust is strong. A frictionally stronger mid-crustal shear zone does not change the overall model behaviors but extension occurred over multiple rolling-hinges. The 3 modes of extension share characteristics similar to geological models proposed to explain the formation of metamorphic core complexes: 1) the crustal flow model for the weak lower crust, 2) the rolling-hinge and crustal flow models when the lower crust is intermediate and 3) the flexural uplift model when the lower crust is strong. Finally we show that the intensity of decoupling between the far field extension and lower crustal flow driven by the regional pressure gradient in the wedge control the overall style of extension in the models.

1. Introduction

The yield strength of the continental lithosphere is primarily constrained by the thermal structure and rheological composition of the lithosphere and is often represented as a yield stress envelope (YSE) (e.g., Burov and Diament, 1995). In extension, its yield strength is such that only when weakened by heating or magmatic processes, a continental lithosphere can breakup (e.g., Buck, 1991; Buck et al., 2005, 2009). For example, Buck (1991) showed that a hot, and therefore weak, orogenic lithosphere with a thick crust is weak enough to stretch in the "wide rift" or "core complex" mode. Some of the best examples of such extensional environments are the Basin and Range province in the western US, Papua New Guinea, and the Aegean.

Several intriguing observations have further driven the search for a more detailed mechanical model for the formation of a rift basin in similarly hot lithosphere including: 1) the lack of variations in crustal thickness over large wavelength, 2) the exhumation of lower crust in metamorphic core complexes (MCCs) and 3) the formation of large-offset low-angle normal fault. The first observation is a key characteristic of the extension of hot lithosphere. Hot ductile lower crust flows to smooth out variations in crustal thickness caused by differential extension (Block and Royden, 1990; McKenzie et al., 2000). Likewise, the topographic gradient in a differentially thickened crust can also drive the flow of ductile lower crust (Braun and Beaumont, 1989; Kruse et al., 1991; Bird, 1991). Several mechanisms were proposed to explain the remaining characteristic observations, i.e., the exhumation of middle crust along shallow-dipping mylonitic shear zone and brittle normal faults (e.g., Gans, 1987; Wernicke, 1981; Buck, 1988; Block and Royden, 1990; Melosh, 1990; McKenzie et al., 2000). The rolling-hinge model proposed that the middle crust is exhumed from large depths by an offset greater than 15 km along a high- or low-angle normal fault rooted in the middle crust (Axen, 1988; Buck, 1988). Other models (Gans, 1987; Block and Royden, 1990; McKenzie et al., 2000) proposed that lower crustal flow caused by local or regional pressure gradients drives exhumation and causes the rotation of an initially high-angle normal fault to a low

* Corresponding author at: Institute for Geophysics, University of Texas at Austin, 10100 Burnet Rd., Austin, TX 78758-4445, United States. Tel.: +1 512 471 0352.
E-mail address: glwu@utexas.edu (G. Wu).

http://dx.doi.org/10.1016/j.epsl.2015.04.005
0012-821X/

angle. Explaining the formation of large-offset normal faults in the rolling-hinge model remains the main issue. Hypotheses include fault strength decreasing with fault offset in a thin brittle upper crust (Buck, 1988; Axen, 1988; Lavier et al., 2000) and stress rotation caused by basal shear or along a weak frictional fault interface (e.g., Yin, 1989; Melosh, 1990). Accordingly, the low dip of a large-offset normal fault can be achieved either through the rotation of a high-angle normal fault (e.g., Buck, 1988) or as a primary fault (e.g., Yin, 1989; Melosh, 1990).

However, in spite of a few exceptions (e.g., Rey et al., 2010), most numerical and theoretical studies of lithospheric extension assumed an initially uniform crustal thickness and ignore regional pressure gradients that would be caused by preexisting variations in crustal thickness. For instance, Buck (1991) showed that a localized mode of crustal extension similar to core complex extension would occur in a uniformly thick lithosphere with weak lower crust. The rolling-hinge model (Buck, 1988; Lavier et al., 1999; Choi et al., 2013) also assumed a lithosphere that initially has a uniform thickness. Following the same mechanical principles with those of the rolling-hinge model proposed by Buck (1988) (i.e., that an active high-angle normal fault is rotated into a low-angle normal fault when exhumed at the surface), sometimes with the addition of melt, numerical models of core complexes forming in a hot and uniformly thick lithosphere with a thick crust have shown that the high-angle rolling-hinge is successful at explaining some of the observations at core-complexes (e.g., Lavier and Buck, 2002; Tirel et al., 2008; Rey et al., 2009; Huet et al., 2011; Gessner et al., 2007). Although successful in explaining the low dip and geometry of normal faults observed at many MCCs, rolling-hinge models failed to explore the combined effects of regional flow due to gradients in crustal thickness (Bird, 1991) and differential stretching (Block and Royden, 1990) on the mechanics of core complex formation. Bialas et al. (2007), Rey et al. (2010), and Whitney et al. (2013) considered the effects of non-uniform crustal and lithospheric thickness but did not analyze the details of the mechanical consequences like the interaction between lower crustal flow and faulting. Huet et al. (2011) used a wedge-shaped layering of the crust without initial topography, Moho relief, or mid-crustal shear zone. In addition, they did not systematically vary the strength of the lower crust.

Another important but often-ignored possibility in lithospheric extension is that a weak mid-crustal shear zone can decouple upper crust from lower crust and mantle. The presence of such a decoupling zone is supported by the inference of the dip of subhorizontal mylonitic shear zone near the base of brittle crust using GPS measurements (Velasco et al., 2010) and by subhorizontal detachment surface detected in seismic reflection profiles such as the S reflector in the Iberia margin (Reston et al., 1996). Even in studies that considered the mechanical effect of a decoupling mid-crustal surface on rifting (e.g., Nagel and Buck, 2006; Lavier and Manatschal, 2006; Huismans and Beaumont, 2011), the crust–mantle boundary and the topography were assumed to be initially flat.

These overlooked components might have substantial influence on the dynamics of lithospheric extension. For instance, it is very likely that the interaction between regional lower crustal flow and normal faulting in a hot lithosphere can result in different extensional styles with single or multiple zones of active basins and ranges. Previous studies of extension (Buck, 1988, 1991; Lavier et al., 2000) have demonstrated that several weakening and hardening phenomena control whether extension in wide rifts stays localized on a single zone (one MCC or graben) or multiple zones (multiple MCCs or grabens) of extension. The loss of cohesion or frictional strength on a fault competes with the resistance of the brittle upper plate to bending (Lavier et al., 2000) to accommodate extension on multiple normal faults rather than on a single normal fault. Viscous strengthening in response to normal faulting at the base of the brittle upper crust can also occur if the lower crust is strong (Lavier and Buck, 2002). In that case, strengthening lead to the formation of multiple normal faults in the upper crust (Lavier and Buck, 2002). At the scale of the lithosphere, thinning of the crust and the associated mantle upwelling strengthen the lithosphere and force deformation to delocalize over multiple extensional centers (Buck, 1991). If the pressure gradient and the strength of the lower crust are such that the lower crust can flow efficiently and smooth out variations in crustal thickness (Buck, 1991) then strengthening due to mantle upwelling is suppressed and extension should continue on one given extensional center or normal fault. When the shear resistance in a high viscosity lower crust opposes flow, it cannot suppress crustal thinning efficiently and as a result mantle upwelling may occur. This mechanism increases the lithosphere's resistance to extension and causes the formation of multiple rift basins (Buck, 1991; Buck et al., 2009).

In this paper, we explore the effects of lower crustal flow driven by a regional pressure gradient on the decoupling of deformation in the lithosphere and the style of rifting that the presence or absence of decoupling generates. Specifically, we conducted numerical experiments on the extension of a two- or three-layer crust in wedge-shaped crust (Fig. 1). We also studied the effects of the composition of the lower crust and included the effect of a preexisting decoupling shear zone at the brittle ductile transition (BDT). While a two-layer division of the crust (upper and lower crust) may be sufficient for most tectonic settings, the presence of a strong gabbroic lowermost lower crust (termed mafic lower crust throughout the paper) has been inferred in some regions, such as the US Cordillera and some parts of the Variscan orogeny in Europe (McGuire, 1994; Müntener et al., 2000). That motivates us to assume a three-layer crust and analyze the effect of a strong gabbroic lower crust on extension mechanisms and styles.

2. Simple analysis of decoupling

We seek to describe the capacity of lower crustal flow driven by a pressure gradient imposed by topographic loading and mantle buoyancy, compared with that driven by far field extension applied at the side of the lithosphere. While the simple analysis presented here ignores the complex non-linear interactions between the brittle and ductile deformation, it is a useful guide to the mechanics of the lithosphere and the interpretation of our numerical models.

2.1. Definition of coupled versus decoupled deformation

Local isostasy occurs when loading or unloading on the lithosphere is counterbalanced at the same location. In contrast, regional isostasy involves the non-local effects such as elastic strength (flexure) and lateral ductile flow over a large distance. Compensation becomes local when the flexural strength of the lithosphere is small so that flexural wavelength is much smaller than the scale of loading and ductile flow is not fast enough (Watts, 2001). In the case of local compensation, brittle deformation in the upper crust is typically compensated by local mantle stretching and upwelling and the deformation appears to be coupled. When the lithosphere has a large flexural rigidity and/or ductile flow is intense, deformation in the brittle upper crust is regionally compensated. Since the regional compensation would involve vigorous lateral flow of the ductile lower crust even for a highly localized deformation of the brittle upper crust (Watts, 2001), the deformation of the upper crust and the mantle lithosphere would appear decoupled.

Here we assume that decoupling and regional compensation occur when the flow rate in the ductile lower crust is greater than

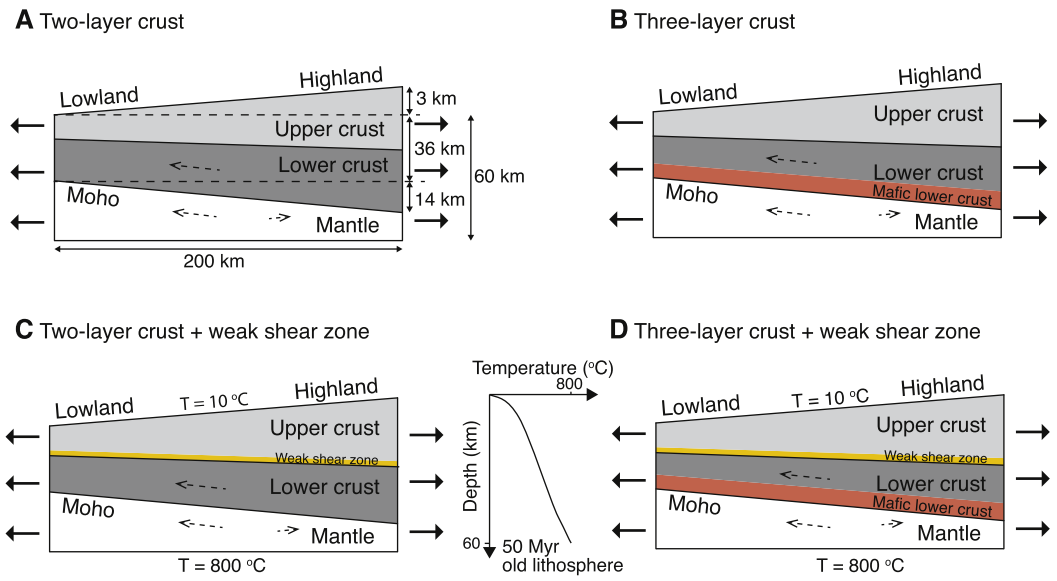

Fig. 1. Model setups. The modeled domain is 200 km wide with overall extension rate of 1.25 cm yr^{-1} (i.e., 0.625 cm yr^{-1} at both sides) for the numerical models. See supplementary Figs. S1 and S2 for temperature and viscosity of the numerical models at very early stage.

the far field boundary conditions. Ductile flow in the lithosphere is generated by horizontal and vertical pressure gradients. The intensity of the flow may exceed the kinematic boundary conditions when excess loading from gradients in crustal thickness are pre-existing. It may also be larger if a weak shear zone or decoupling surface is present at the BDT. Another very important factor controlling the rate of ductile flow is the variation in channel thickness in the lower crust (McKenzie et al., 2000). For example, if the channel thickness decreases in the direction of the flow, the flow rate increases in order to conserve mass.

2.2. Decoupling ratio

We provide a simple analysis of the effect of lower crustal viscosity and loading from topography and Moho relief on the decoupling of the deformation. We ignore the effects of both channel thickness and weak shear zones for simplicity. Lower crustal flow occurs along the width of the lithosphere, W, along the BDT along a surface of length $W/\cos\alpha$ and along the Moho along a surface of length $W/\cos\beta$, where α is the slope angle of BDT and β is the slope angle of the Moho, and both are small, i.e., <5–10°. We propose that the intensity of decoupling of lower crust with respect to upper crust and mantle can be roughly expressed as the ratio (D) of the mean horizontal velocity ($\bar{u}$) of the pressure gradient-driven channel flow in the lower crust to the boundary velocity (v_x). If the channel velocity is significant (i.e., $D \geq 1$) then the deformation is decoupled while coupled if the channel velocity is negligible (i.e., $D \ll 1$).

In a wedge-shaped crust where both regional topography and Moho relief are present (Fig. 1) and the BDT is assumed to be sub-horizontal, the pressure gradient along the base of wedge-shaped brittle crust is (Bird, 1991):

$$\nabla P_x^{topo} \approx \rho_c g \frac{\partial h_t}{\partial x} \cos\alpha \approx \rho_c g \frac{\partial h_t}{\partial x} \tag{2}$$

where ρ_c is the averaged density of upper crust, g the gravity, $\partial h_t/\partial x$ the gradient of topography and $\cos\alpha \approx 1$ ($\alpha < 10°$).

Similarly, a contribution from the Moho relief to the pressure gradient in the lower crust is:

$$\nabla P_x^{moho} \approx (\rho_m - \rho_c) g \frac{\partial h_m}{\partial x} \cos\beta \approx (\rho_m - \rho_c) g \frac{\partial h_m}{\partial x} \tag{3}$$

where h_m is the Moho relief and $\cos\beta \approx 1$ ($\beta < 10°$). The mean velocity in the lower crust is:

$$\bar{u} = \frac{h^2}{12\eta_{lc}} \left(\nabla P_x^{moho} - \nabla P_x^{topo} \right) \tag{4}$$

where h is the channel thickness and η_{lc} is the viscosity of lower crust. The decoupling ratio D is defined as:

$$D = \frac{|\bar{u}|}{v_x} = \frac{h^2}{12\eta_{lc} v_x} |\nabla P_x| = \frac{h^2 g}{12\eta_{lc} v_x} \left| \rho_c \frac{\partial h_t}{\partial x} + (\rho_m - \rho_c) \frac{\partial h_m}{\partial x} \right| \tag{5}$$

We proceed to compute D using Eq. (5) for a 200 km-wide crustal wedge. We assumed a topographic relief of 3 km and a corresponding Moho relief of 14 km under local isostasy (Fig. 1A). The decoupling factor, D, is plotted with respect to viscosity of the lower crust ranging 10^{19}–10^{23} Pa s and for 3 values of channel thickness (10 km, 20 km and 30 km) (Fig. 2). The plot shows that D decreases markedly as the lower crust's viscosity increases. D is nearly negligible when the viscosity is greater than 10^{21} Pa s regardless of the channel thickness. The plot also shows that when the thickness of the channel increases, the degree of decoupling would increase. The simple analysis presented in Fig. 2 suggests that the viscosity and thickness of the lower crust has to be smaller than $\sim 10^{20}$ Pa s and greater than 10 km, respectively, to allow for significant decoupling. A sufficiently large pressure gradient may cause deformations other than the lower crustal flow but such a case is beyond the premises of this simple calculations. Varying the width of the lithosphere (W) from 100 km to 300 km, the topographic relief from 1 km to 5 km, and correspondingly Moho relief from 5 km to 24 km (local compensation) generates a maximum topographic and Moho gradient of 5.7° and 13° respectively. These values still allow us to make the same approximations as in Eq. (5). Therefore changing the wedge geometry in this range of dimensions does not significantly affect the decoupling analysis.

2.3. Factors contributing to decoupling

Several other factors will play a significant role on the decoupling ratio: 1) The thinning of the lower crustal channel from high to low elevation (Fig. 1) contributes significantly to the intensity

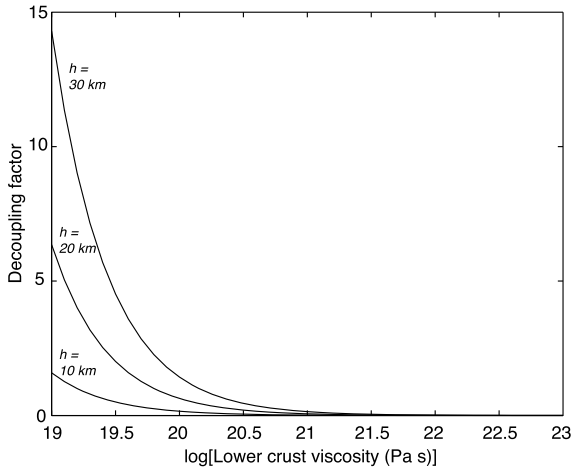

Fig. 2. Intensity of decoupling induced by topographic loading and mantle buoyancy as a function of viscosity, η_{lc}, and thickness, h, of the lower crustal channel.

of lower crust flow. As the lower crust enters a thinner channel the intensity of the flow increases so that mass is conserved. As a result the decoupling ratio should increase significantly as strain rate increases. 2) When present, the weak shear zone at the BDT is a very narrow channel with low viscosity ($\sim 10^{19}$ Pa s at ~300–400 °C). Our simple analysis cannot take these parameters into account. We therefore run numerical experiments to analyze the effect of lower crustal strength and the presence of a weak mid-crustal shear zone.

The existence of mid-crustal shear zones is supported by geological and geophysical evidence (e.g., Jolivet et al., 1998; Lister and Davis, 1989) and numerical models (e.g., Lavier and Manatschal, 2006; Regenauer-Lieb et al., 2006). One difficulty, however, is to differentiate preexisting shear zones from the ones developed during extension. Here we choose to consider that mid-crustal shear zones always exist in the crust; however, they may be weak, strong, or even completely annealed depending on the geological conditions. To incorporate a full dynamic evolution of the shear zone during extension is out of the scope of this work. Finally when the weak shear zone behaves in a brittle manner whether it slips or not depends on its cohesional and frictional strengths. We will also analyze the effects of the shear zone frictional strength.

3. Model setup

Both regional scale flow (Bird, 1991) and flow driven by emerging differential crustal thickness (Block and Royden, 1990) are simulated in our models (Figs. 1 and 3). The mechanism for normal faulting used in the models follows an elasto-plastic constitutive update with a Mohr–Coulomb yield criterion (Lavier et al., 1999, 2000) that is consistent with Andersonian fault mechanics (Anderson, 1951). We decreased the fault strength as a function of plastic strain to simulate weakening of the normal faults (Lavier and Buck, 2002; Lavier and Manatschal, 2006). We present experiments with and without preexisting decoupling shear zone. In both sets of experiments we explore the effect of the lower crustal strength as a function of rheological composition (Fig. 3). We investigated a two-layer division of the crust using two sets of models (Fig. 3A and B, with and without a decoupling layer, respectively) as well as a three-layer crustal structure with two sets of models (Fig. 3C and D). Finally, the numerical models are compared to continental extension in several regions around the world to test whether they are developing patterns of deformation that are similar to those observed in natural examples.

We limited the number of numerical experiments and computing time by choosing fixed dimensions and initial thermal structure for the lithosphere that correspond to the wedge described in Fig. 1A. We set the thermal age of the lithosphere at 50 Myr with a constant geotherm to set the initial thermal structure. We tested bottom boundary temperature from 600 °C to 1000 °C with an interval of 50 °C in our early simulations. The changes of the bottom boundary temperature in the range only slightly affect our models. Moreover a temperature of 700–800 °C matches best the geotherm imposed by the thermal age of 50 Myr. We used constant boundary temperatures at the bottom (800 °C) and surface (10 °C) and zero heat flux boundary conditions for the sides of the model for all the numerical experiments presented here. Fig. 3 shows the initial lithospheric strength profile corresponding to parameters given in Table 1. To avoid mesh errors at the surface, a very small amount of erosion and sedimentation are simulated to avoid the development of sharp corners and overhangs. We applied divergent boundary conditions on the sides with a constant overall speed of 1.25 cm yr^{-1}. To simulate regional isostasy we use a Winkler foundation at the base of the models.

The decoupling layer is modeled as a thin (~2 km) shear zone at the base of upper crust in models with two- and three-layer crust (Fig. 1B and D), respectively. It is initially behaving in a ductile manner and is assumed to have low viscosity ($\sim 10^{19}$ Pa s at ~300–400 °C, see supplementary Figs. S1A, C and S2). When the shear zone is included (Fig. 1B and D), we varied its frictional strength from very weak to very strong with frictional angle, θ, ranging from 5° to 25° when it enters the brittle field.

The rheology of the lower crust is difficult to specify because it depends on the mineral composition, grain size, thermal struc-

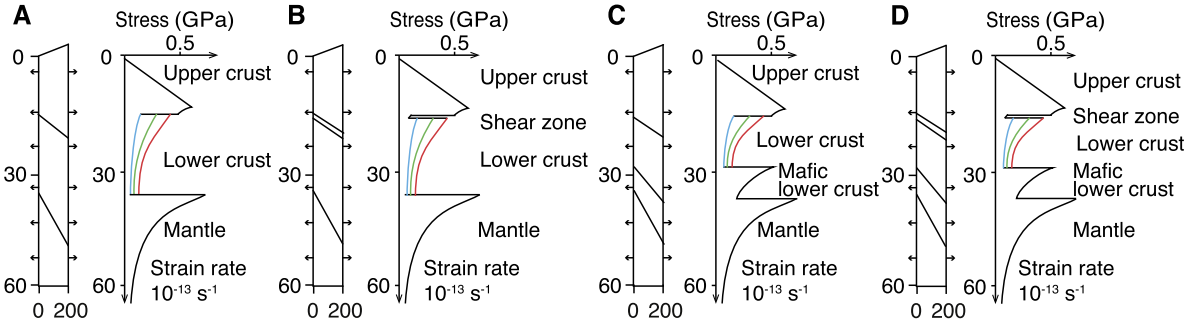

Fig. 3. Strength envelope for the crust and lithospheric mantle. The model domain is 200 km wide with a 60 km thickness at left side and additional 3 km topography at the right side. A, B: A two-layer crust and plagioclase rheology (Ranalli, 1995) for the upper crust, dry quartz, wet quartz, and wet quartz added with 0.12% water (Jaoul et al., 1984) for strong, intermediate, and weak lower crust (red, green, and blue curve in the strength envelope), respectively, and olivine for the mantle (Kirby and Kronenberg, 1987). C, D: A three-layer crust and plagioclase rheology (Ranalli, 1995) for the upper crust, plagioclase (Ranalli, 1995), weakened plagioclase and strongly weakened plagioclase for strong, intermediate and weak lower crust (red, green, and blue curve in the strength envelope), respectively, strengthened plagioclase (Ranalli, 1995) for the mafic lower crust, and olivine for the mantle (Kirby and Kronenberg, 1987). The shear zone in B and D is ~2 km thick, and is of low viscosity when ductile, and low frictional angle (θ_s, 5°–25°) when brittle. See Table 1 for detailed parameters.

Table 1
Summary of model parameters.

Phase	ρ (kg m^{-3})	θ (°)	θ' (°)	C (MPa)	A (MPa^{-n} s^{-1})	E_a (J mol^{-1})	n	C_p (J kg^{-1} K^{-1})	h_r (W kg^{-1})
Upper crust	2700	30	15	40	0.125	2.76×10^5	3.05	1000	10^{-9}
Weak lower crust (2-layer crust)	2800	30	15	40	2.5×10^{-3}	1.63×10^5	1.8	1000	10^{-9}
Intermediate lower crust (2-layer crust)	2800	30	15	40	1.85×10^{-6}	1.63×10^5	2.8	1000	10^{-9}
Strong lower crust (2-layer crust)	2800	30	15	40	1.37×10^{-6}	1.84×10^5	2.8	1000	10^{-9}
Weak lower crust (3-layer crust)	2800	30	15	40	0.125	1.8×10^5	3.05	1000	10^{-9}
Intermediate lower crust (3-layer crust)	2800	30	15	40	0.125	2.4×10^5	3.05	1000	10^{-9}
Strong lower crust (3-layer crust)	2800	30	15	40	0.125	2.76×10^5	3.05	1000	10^{-9}
Mafic lower crust (3-layer crust)	3000	30	15	40	0.125	3.5×10^5	3.05	1000	10^{-9}
Mid-crustal shear zone	2800	5–25	5–25	4	0.125	1.76×10^5	3.05	1000	10^{-9}
Mantle	3300	30	15	40	7.0×10^4	5.2×10^5	3.0	1000	–

Abbreviation in column headings: ρ (density), θ (initial frictional angle), θ' (frictional angle after weakening), C (cohesion), A (coefficient in the creep law), E_a (activation energy in creep law), n (exponential component in the creep law), C_p (heat capacity), h_r (radioactive heating).
See caption of Fig. 3 for references.

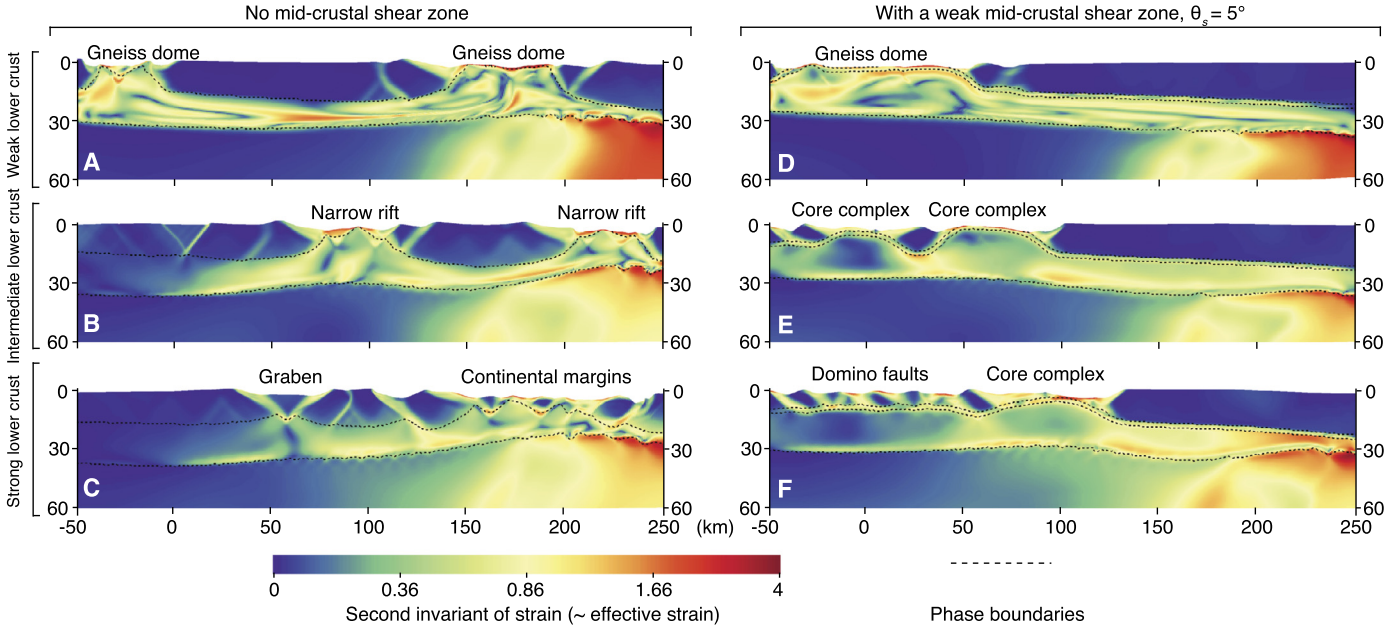

Fig. 4. Second invariant of strain (i.e. effective strain) of the numerical models with a 2-layer crust, without (A–C) and with (D–F) a mid-crustal weak shear zone. The shear zone friction angle is 5°. All the models are shown at 50% extension corresponding to a stretching factor $\beta = 1.5$ after 8 Myr of evolution. See also Mov. 1–3 corresponding to D–F, respectively, and supplementary Figs. S3 and S4 for corresponding temperature and effective viscosity.

ture and the presence/absence of fluids/magmas. For each setup in Fig. 1, we varied the rheology of the lower crust from low to high viscosity (Fig. 3) to study its effect on the intensity of lower crustal flow and decoupling of the deformation between crust and mantle lithosphere. In models with a two-layer crust, we use the creep law for dry quartz, wet quartz, and wet quartz with 0.12% added water (Jaoul et al., 1984) for strong (high viscosity), intermediate (low viscosity), and weak (minimum viscosity) lower crust (red, green, and blue in Fig. 3A and B), respectively. In models with a three-layer crust, we used creep law for plagioclase (Ranalli, 1995) as a reference, and systematically reduced the activation energy term in the creep law, so that lower crustal viscosity varied from high for cold crust to the minimum viscosity for hot crust (red, green, and blue in Fig. 3C and D), respectively.

We used a modified version of PARAVOZ (Poliakov et al., 1993; Tan et al., 2012) to carry out the numerical modeling. We used a fine mesh of 500 m by 500 m. We mainly varied the viscosity of the lower crust, and the frictional strength of the mid-crustal shear zone if included. All the other parameters are kept the same across all the models (Table 1).

4. Results

4.1. 2-Layer models

After 50% of extension models without (Fig. 4A–C) and with (Fig. 4D–F and Mov. 1–3) a mid-crustal shear zone show that mantle upwelling is more intense on the highland side of the models (zone of high strain in red), and that as lower-crustal strength increases the extensional style changes from lower-crustal exhumation dominated to upper-crustal faulting dominated. In models with no mid-crustal shear zone (Fig. 4A–C), brittle deformation does not necessarily focus in the thin part of upper crust and even tend to break the highland part of the model. In contrast, when a weak mid-crustal shear zone is present, upper-crustal deformation always starts in the lowland (Fig. 4D–F).

With a weak lower crust (Fig. 4A) but no mid-crustal shear zone, lower crustal exhumation in a ~50 km wide gneiss dome dominates the deformation pattern. It generates symmetric a gneiss dome flanked by two active normal faults. For intermediate strength lower crust (Fig. 4B), thinning of the crust is more closely related to mantle upwelling as indicated by the upwardly warped

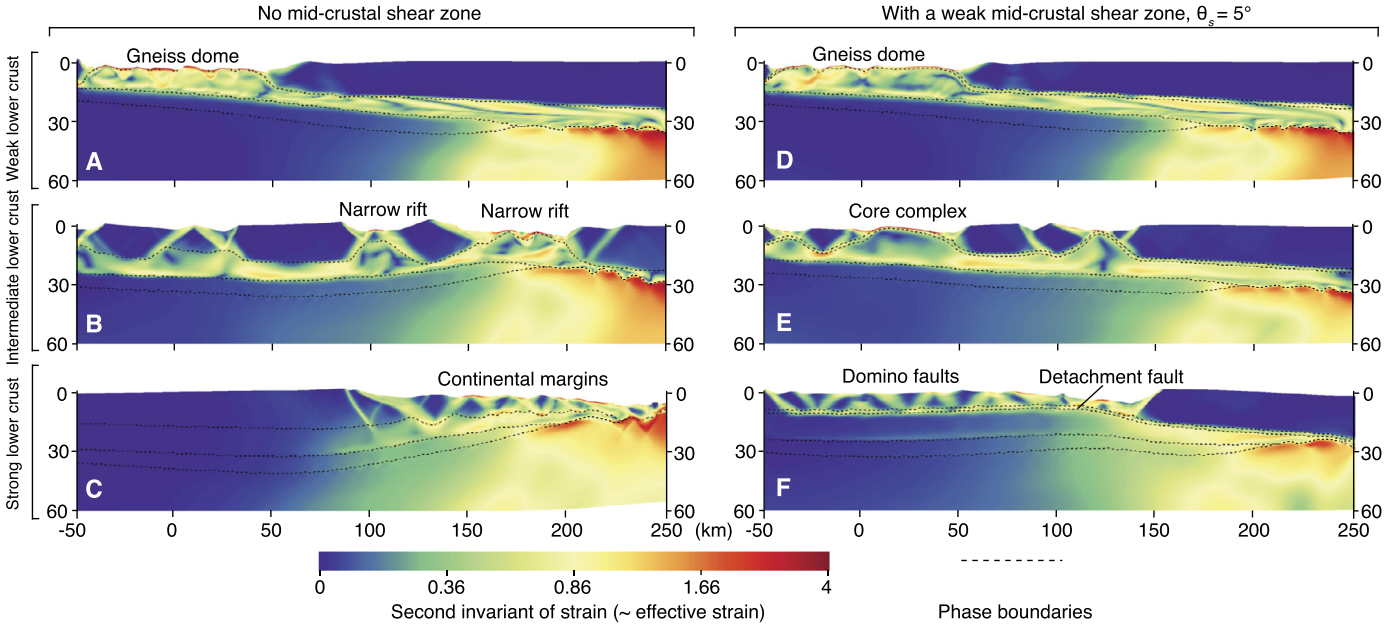

Fig. 5. Second invariant of strain (i.e., effective strain) of the 3-layer models without (A–C) and with (D–F) a mid-crustal weak shear zone. The shear zone friction angle θ_s is 5°. The deformation style is very similar to that described in Fig. 4, with the exception of case A (see text for detailed explanation). All the models are at 50% extension (i.e., stretching factor $\beta = 1.5$) with 8 Ma of extension at 1.25 cm yr^{-1}. See supplementary Figs. S5 and S6 for corresponding temperature and effective viscosity.

Moho. In this case, the isostatic response renders the gneiss dome (Fig. 4B) similar to a narrow rift exhuming lower crustal material. With a strong lower crust (Fig. 4C), a series of adjacent half-grabens develop over the upwelling mantle and connect together to form a structure similar to a thinned continental margin.

When the mid-crustal shear zone is present (Fig. 4D–F and Mov. 1–3) upper crustal deformation for the weak to intermediate strength lower crust develops rolling-hinge normal faults exhuming lower crust in structures similar to MCCs (Buck, 1988). However, when the lower crust is weak, one single very wide (~100 km) gneiss dome forms (Fig. 4D) and lower crustal flow forms a symmetric pattern of exhumation. For a stronger lower crust (Fig. 4E), two core complexes 30 km and 50 km wide form separated by major crustal blocks, deformation is more asymmetric and strain in the lower crustal flow is less intense. When the lower crust is strong (Fig. 4F) a single 50 km wide core complex forms. However more distributed extension occurs in the upper crust forming a thin crustal layer on top of the exhuming and upwelling lower crust and a zone of highly extended upper crust with domino style faulting develops over the mid-crustal shear zone (Fig. 4F).

4.2. 3-Layer models

The models with a three-layer crust behave similarly to the two-layer crust models (Fig. 5). One apparent difference is that, when the mid-crustal shear zone is absent and the lower crust is very weak (Fig. 5A), continuous exhumation of lower crust occurs along a large offset normal fault in a way similar to that predicted by the rolling hinge model (e.g., Buck, 1988; Lavier et al., 1999; Choi et al., 2013). The corresponding 2-layer model (Fig. 4A) produces symmetric massifs bounded by high-angle normal faults. When compared to models in Fig. 4 (2-layer models), the Moho is exhumed to 15 km depth in cases A, B, D and E (Fig. 5) showing that crustal thinning is more intense. Crustal thinning is particularly intense in the model 5C (Fig. 5C) where crustal stretching and mantle upwelling thin the crust to less than 3 km. Finally, in all the 3-layer models (Fig. 5), the strong mafic lower crust is thinned to a negligible thickness under the highland where mantle upwelling is largest.

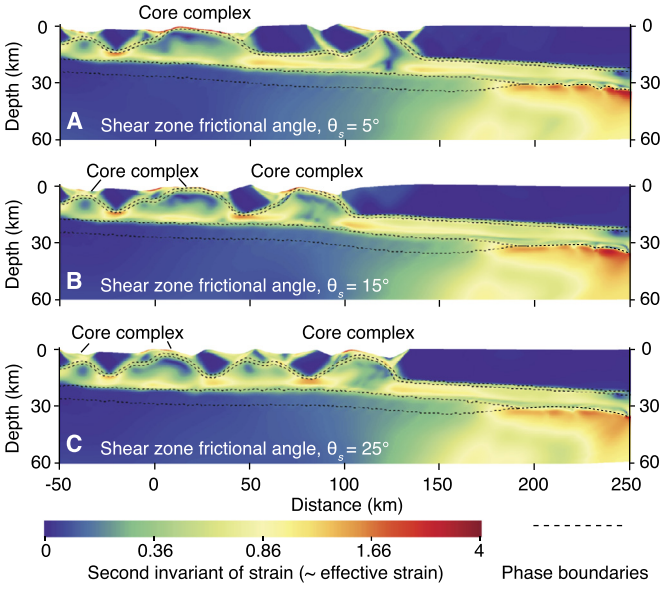

Fig. 6. Second invariant of strain (i.e., effective strain) from 3-layer models with the intermediate-strength lower crust and the mid-crustal shear zones. The shear zone frictional angle, θ_s, is A. 5°, B. 15°, and C. 25°. All the models are at 50% extension (i.e., stretching factor $\beta = 1.5$) with 8 Ma of extension at 1.25 cm yr^{-1}. See supplementary Figs. S7 and S8 for corresponding temperature and effective viscosity.

4.3. Effects of the frictional strength of the mid-crustal shear zone

The internal friction angle of the mid-crustal shear zone was changed from 5° to 15° and 25°. As expected, Fig. 6A is identical to Fig. 5E since the same parameters are used in both simulations. However, as θ increases (15°, and 25° for Fig. 6B and C, respectively), more core complexes form but they are narrower (from 70 km to 20 km wide). All other parameters being constant, as the frictional strength of the mid-crustal shear zone increases, we find

that extension is more distributed and results in the formation of multiple closely spaced rolling hinges with normal faults accumulating smaller offsets. Not all core complexes exhume lower crust to the surface and the deformation migrates towards the highland with increasing extension similar as shown in Mov. 2.

5. Discussions

5.1. Effects of the lower crustal strength

5.1.1. In the absence of a weak mid-crustal shear zone

The models without a preexisting shear zone show systematic changes with increasing strength of the lower crust (Figs. 4A–C and 5A–C) in terms of the spacing of extensional centers, normal fault offsets, and style of rifts and half grabens. Transition from localized to distributed deformation encapsulates the main change associated with increasing lower crustal strength. As a result, the number of small offset normal faults increases and they accommodate a greater proportion of total extension as the lower crust gets stronger. Finally, increasing viscosity of the lower crust decreases the degree of decoupling (Eq. (5)).

In the 3-layer models, the presence of a high viscosity mafic lower crust increases lower crustal strength. As a result the strength of the lithosphere allows for the formation of a thinner viscous channel. According to our channel flow-based analysis (Fig. 2), the reduction in channel thickness, l, allows for more coupling. However in the outlier case (Fig. 5A), even though the channel thickness is smaller, the lower crustal viscosity is so low that the upper crustal deformation appears decoupled (Fig. 2) and a large massif exhuming lower crust forms in the low land. In the other cases, coupling across a thin lower crustal channel leads to more intense and focused crustal thinning, which also implies that compensation is more local. In this framework of degree of decoupling, hardening of the lithosphere is supposed to determine whether deformation stays localized on one large-offset fault or is distributed over multiple faults. Therefore, processes such as crustal thinning, viscous strengthening of the lower crust due to increased strain rates and bending of the upper crust are likely to dominate the deformation processes as was proposed by Buck et al. (1999).

5.1.2. Effects of the weak mid-crustal shear zone

The inclusion of a weak mid-crustal shear zone (frictional angle, $\theta_s = 5°$ and viscosity of 10^{19} Pa s when ductile, at ~300–400 °C, see supplementary Figs. S1–S2) makes the crust accommodate extension more by lower-crustal flow rather than upper-crustal faulting (Figs. 4D–F, 5D–F). All six models in Figs. 4D–F and 5D–F develop large-offset low-angle normal faults. The extension is generally decoupled (Figs. 4D–F, 5D–F and Mov. 1–3) and the regional lower crustal flow from thick to thin crust is intense. Common to all models is the regional migration of the deformation from thin to thick crustal domains and the formation a model-wide subhorizontal Moho discontinuity (Mov. 1–3, corresponding to Fig. 4D–F). The weak mid-crustal shear zone is highly effective in decoupling upper crustal and mantle lithosphere deformation and thus significantly enhances lower crustal flow, smoothing out the crustal relief generated by thinning in all cases.

When the mid-crustal shear zone is present, strength of the lower crust determines the distance up to which thinning of brittle upper crust propagates. For instance, the brittle deformation always starts from the thinnest part but it appears to stop propagating towards the highland at 75, 100 and 125 km in the 2-layer models with weak, intermediate and strong lower crust (Fig. 4D–F). This correlation must reflect the balance between increase in brittle strength towards the thicker portion of the crustal wedge and viscous stress involved in the flow of lower crust. When the lower crust is weak, the associated viscous stress must be comparable to the brittle strength of the upper crust at the distance of 75 km; when the lower crust is strong, the viscous stress must be as large as the brittle strength of the thicker portion of upper crustal at the distance of 125 km. Although not as clear as in the 2-layer models, the same trend is found in the 3-layer models (Fig. 5D–F) and the distance traveled by deformation front toward the highland is overall greater compared to that of the corresponding 2-layer model. Lower degree of decoupling due to the smaller channel thickness of the 3-layer models can explain this difference.

Both weak ductile crust and the mid-crustal shear zone favor decoupled extension of a wedge shaped crust. However, decoupled extension would require a very weak ductile crust without a mid-crustal shear zone. The results are in agreement with our simple analysis (Fig. 2). While both weak shear zone and weak lower crust can decouple the brittle upper crust from the lower crust, a shear zone is particularly effective in facilitating sub-horizontal shear flow and inducing decoupling in the crustal wedge.

5.1.3. Style of MCC formation

The models suggest that the strength of the lower crust controls the style of MCC formation. We found that extension with a weak lower crust favors symmetrical structures similar to gneiss domes in which extension is accommodated by ductile flow while extension with a stronger lower crust leads to the formation of asymmetric MCCs in which extension is accommodated by both ductile flow and distributed stretching over a detachment surface.

The mechanism of the formation of gneiss domes in the models with weak lower crust (Figs. 4D and 5D) corresponds to the crustal flow or intracrustal isostasy model proposed by Gans (1987) and Block and Royden (1990). Gneiss domes indicating extrusion of deep lower crust by such a process have been observed in the Menderes massif, Turkey (Hetzel et al., 1995; Gessner et al., 2001), NW Rhodope, the Aegean (Gautier et al., 1999), and Papua New Guinea (Martinez et al., 2001). Intermediate strength of lower crust appears to produce MCCs by the rolling-hinge mechanism (Figs. 4E, 5E, and Fig. 6) and exhumes lower crust to the surface (Lavier et al., 1999; Choi et al., 2013). The process of MCC formation in the strong lower crust models (Figs. 4F and 5F) would correspond to the flexural uplift model (Spencer, 1984), in which stretching of the upper crust over a flowing and thickening lower crust eventually leads to the exhumation of lower crust. This model is still used to explain core complexes similar to the Whipple Mountains in the Basin and Range province (Spencer, 1984).

The main characteristics of Cenozoic tectonics in the Basin and Range and the Aegean are: 1) that both systems were young orogenic belts at the initiation of extension (Wernicke, 1985; Jolivet and Brun, 2010), 2) that they both developed core complexes (Davis and Coney, 1979; Coney et al., 1980; Jolivet and Brun, 2010), and 3) that the Moho is rather continuous and regionally subhorizontal (Klemperer et al., 1986; McCarthy et al., 1991) in the extended region. The numerical models including a weak mid-crustal shear zone (Figs. 4D–F, 5D–F, 6A–C) do fit well with these general features. The numerically produced detachment structure is also in agreement with those observed in the thermally re-equilibrated lithosphere, such as the Norwegian margin (Osmundsen and Ebbing, 2008), Iberia margin (e.g., Reston et al., 1996), and South China Sea (e.g., McIntosh et al., 2014).

The migration of extension seems to conform to the Death Valley region (Miller and Pavlis, 2005), which is comparative in scale, and the Elba to the Adriatic coast (Barchi et al., 1998). However it should be bear in mind that our model might still be in a local-regional scale compared to the Aegean and the Basin and Range. In addition we did not consider arc migration, magma generation, and delamination, which may affect the migration of extension, and may compete with our implied conditions.

5.2. Modes of extension of wedge-shaped crust

We found that the lithospheric wedge extends in one of the following two ways: (1) by lower crustal flow, crustal and mantle lithosphere thinning in response to the extension applied at the model boundaries, (2) by intense extension of the highland and the associated upward flow of asthenosphere to compensate for flow of lower crust towards the lowland.

The intensity of lower crustal flow is mainly controlled by the strength of the lower crust and the presence of a weak mid-crustal shear zone at the BDT in the crust. The mid-crustal shear zone is weaker than the lower crust, and when the lower crust is weak (wet quartz rheology) as well, lower crustal flow is intense. As a result, upper crustal extension is localized and accommodated by the exhumation of lower crust to the surface as seen in Figs. 4D–E, 5D–E and 6A–C. These behaviors are also characteristics of intracrustal isostasy (e.g., Block and Royden, 1990). When lower crustal flow is less intense, extension is accommodated by distributed brittle deformation in the upper crust such as domino style faulting (Figs. 4F and 5F), which in turn indicates upward warping of a detachment fault by mostly vertical flow of the lower crust (Spencer, 1984). Upper crustal deformation migrating toward the highland seen in our models with a weak mid-crustal shear zones (Fig. 4D–F, Fig. 5D–F, 6A–C) are reminiscent of passive margins like Iberia (Ranero and Pérez-Gussinyé, 2010; Reston et al., 1996; Nagel and Buck, 2006). Finally the weak mid-crustal shear zone predominantly records sub-horizontal simple shear as is typically observed in mylonitic shear zones at MCCs (e.g., Spencer, 1984). Because these characteristics persist even when the shear zone behave in a brittle manner (Fig. 6 and supplementary Figs. S4, S6 and S8) we believe that it behaves in a way akin to a detachment fault (Davis and Lister, 1988).

5.3. Implications for the continental margin development

The Atlantic margins developed in Caledonian to Variscan orogenic belts (Reston et al., 1996; Lavier and Manatschal, 2006) show 1) multiple tilted high-angle normal fault blocks and few detachment faults, 2) the thinning of the crust compensated in the mantle, and 3) the convex upward Moho that is even exhumed at the seafloor in some places. These characteristics agree with the coupled extension that occurred in our models with strong lower crust and without a mid-crustal shear zone (Figs. 5B–C and 6B–C). These conditions might be realized in cooler lower lithosphere of long-lived orogenic belts and annealed mid-crustal shear zone inherited from the previous orogenesis. The modeling results also suggest that the presence of reflectors (S reflector in Iberia, Reston et al., 1996) interpreted as detachment at passive margins is not a pre-existing weak mid-crustal shear zone but rather the result of shear and thinning at the brittle ductile transition as suggested by Lavier and Manatschal (2006).

6. Summary

A wedge shape of crust at the beginning stage of extension is an often-ignored possibility in numerical models. We studied the influence of mid-crustal shear zone and lower crustal strength on the extension of a wedge-shape crust using two-dimensional numerical models. When there is a weak mid-crustal shear zone, we identify three distinct modes of extension determined by the strength of the lower crust, which are characterized by: 1) significant exhumation of lower crust that leads to the formation of massifs in the weak lower crust models, 2) rolling-hinges with large offset faults in the models with intermediate-strength lower, and finally 3) intensive domino style normal faulting and negligible thinning of the lower crust in the case of the models with strong lower crust. This result shows that different types of core complex may form in a crustal wedge and that the different models for the formation of core complexes (e.g., Buck, 1988; Block and Royden, 1990; Axen, 1988) are not mutually exclusive and are representative of a change in the strength and intensity of lower crustal flow versus upper crustal faulting in the wedge. A frictionally stronger mid-crustal shear zone does not change the overall model behaviors but extension occurred over multiple rolling-hinges. Without the mid-crustal shear zone, transition from localized to distributed deformation style occurs as lower crustal strength increases. The associated changes include decrease in the spacing of extensional centers, decrease in offsets and increase in number of normal faults, and transition of regional to local isostatic compensation. These changes lead to the formation of structure similar to those observed at highly extended non-volcanic continental margins (e.g. Ranero and Pérez-Gussinyé, 2010).

Our numerical models cover a wide range of continental extensions observed around the world, and have promising applications. We propose that the presence of a mid-crustal shear zone at the base of the upper crust focuses shear flow subhorizontally in a way similar to what is inferred for a décollement. Finally we show that the styles of extension in a crustal wedge are dependent on the ratio, D of rate of lower crustal flow to the far field rate of extension. As explained above, this ratio depends strongly on lower crustal strength and the potential presence of a weak mid-crustal shear zone at the brittle ductile transition. This additional parameter allows us to capture the combined influence of the temperature, viscosity, rate of extension and initial lithospheric structure into one non-dimensional number, D. When D is large enough, extension in the upper crust is compensated by lateral flow of lower crust, which corresponds to regional isostasy. If D is small, local isostasy becomes dominant, in which on-site crustal thinning and mantle upwelling compensate extension in the upper crust.

Acknowledgements

We are grateful to Patrice Rey and Loic Labrousse for constructive comments that helped to improve the paper, and Editor Yanick Ricard for helpful assistance. This work was supported in part by the Academic Excellence Alliance program award to Luc L. Lavier from King Abdullah University of Science and Technology (KAUST) Global Collaborative Research under the title “3-D numerical modeling of the tectonic and thermal evolution of continental rifting”. This is UTIG contribution 2842.

Appendix A. Supplementary material

Supplementary material related to this article can be found online at http://dx.doi.org/10.1016/j.epsl.2015.04.005.

References

Anderson, E.M., 1951. The Dynamics of Faulting, 2nd ed. Oliver and Boyd, Edinburgh.
Axen, G.J., 1988. The geometry of planar domino-style normal faults above a dipping basal detachment. J. Struct. Geol. 10, 405–411.
Barchi, M.R., Minelli, G., Pialli, G., 1998. The crop 03 profile: a synthesis of results on deep structures of the Northern Apennines. Mem. Soc. Geol. Ital. 52, 383–400.
Bialas, R.W., Buck, W.R., Studinger, M., Fitzgerald, P.G., 2007. Plateau collapse model for the Transantarctic Mountains–West Antarctic Rift System: insights from numerical experiments. Geology 35, 687–690.
Bird, P., 1991. Lateral extrusion of lower crust from under high topography in the isostatic limit. J. Geophys. Res. 96, 10275–10286.
Block, L., Royden, L.H., 1990. Core complex geometries and regional scale flow in the lower crust. Tectonics 9, 557–567.
Braun, J., Beaumont, C., 1989. A physical explanation of the relation between flank uplifts and the breakup unconformity at rifted continental margins. Geology 17, 760–764.
Buck, W.R., 1988. Flexural rotation of normal faults. Tectonics 7, 959–973.

Buck, W.R., 1991. Modes of continental lithospheric extension. J. Geophys. Res. 96, 20161–20178.
Buck, W.R., Lavier, L.L., Poliakov, A.N., 1999. How to make a rift wide. Philos. Trans. R. Soc. Lond. A 357, 671–693.
Buck, W.R., Lavier, L.L., Poliakov, A.N., 2005. Modes of faulting at mid-ocean ridges. Nature 434, 719–723.
Buck, W.R., Small, C., Ryan, W.B.F., 2009. Constraints on asthenospheric flow from the depths of oceanic spreading centers: the East Pacific Rise and the Australian–Antarctic Discordance. Geochem. Geophys. Geosyst. 10, Q09007.
Burov, E.B., Diament, M., 1995. The effective elastic thickness (Te) of continental lithosphere: what does it really mean? J. Geophys. Res. 100, 3905–3927.
Choi, E., Buck, W.R., Lavier, L.L., Petersen, K.D., 2013. Using core complex geometry to constrain fault strength. Geophys. Res. Lett. 40, 3863–3867.
Coney, P.J., Jones, D.L., Monger, J.W., 1980. Cordilleran suspect terranes. Nature 288, 329–333.
Davis, G.H., Coney, P.J., 1979. Geologic development of the Cordilleran metamorphic core complexes. Geology 7, 120–124.
Davis, G.A., Lister, G.S., 1988. Detachment faulting in continental extension: perspectives from the southwestern US Cordillera. Spec. Pap., Geol. Soc. Am. 218, 133–160.
Gans, P.B., 1987. An open-system, two-layer crustal stretching model for the Eastern Great Basin. Tectonics 6, 1–12.
Gautier, P., et al., 1999. Timing, kinematics and cause of Aegean extension: a scenario based on a comparison with simple analogue experiments. Tectonophysics 315, 31–72.
Gessner, K., et al., 2001. An active bivergent rolling-hinge detachment system: central Menderes metamorphic core complex in western Turkey. Geology 29, 611–614.
Gessner, K., Wijns, C., Moresi, L., 2007. Significance of strain localization in the lower crust for structural evolution and thermal history of metamorphic core complexes. Tectonics 26.
Hetzel, R., Passchier, C.W., Ring, U., Dora, Ö.O., 1995. Bivergent extension in orogenic belts: the Menderes massif (southwestern Turkey). Geology 23, 455–458.
Huet, B., Le Pourhiet, L., Labrousse, L., Burov, E.B., Jolivet, L., 2011. Formation of metamorphic core complex in inherited wedges: a thermomechanical modelling study. Earth Planet. Sci. Lett. 309, 249–257.
Huismans, R., Beaumont, C., 2011. Depth-dependent extension, two-stage breakup and cratonic underplating at rifted margins. Nature 473, 74–78.
Jaoul, O., Tullis, J., Kronenberg, A., 1984. The effect of varying water contents on the creep behavior of Heavitree quartzite. J. Geophys. Res. 89, 4298–4312.
Jolivet, L., et al., 1998. Midcrustal shear zones in postorogenic extension: example from the northern Tyrrhenian Sea. J. Geophys. Res. 103, 12123–12160.
Jolivet, L., Brun, J.P., 2010. Cenozoic geodynamic evolution of the Aegean. Int. J. Earth Sci. 99, 109–138.
Kirby, S.H., Kronenberg, A.K., 1987. Rheology of the lithosphere: selected topics. Rev. Geophys. 25, 1219–1244.
Klemperer, S.L., Hauge, T.A., Hauser, E.C., Oliver, J.E., Potter, C.J., 1986. The Moho in the northern Basin and Range province, Nevada, along the COCORP 40 N seismic-reflection transect. Geol. Soc. Am. Bull. 97, 603–618.
Kruse, S., McNutt, M., Phipps-Morgan, J., Royden, L., Wernicke, B., 1991. Lithospheric extension near Lake Mead, Nevada: a model for ductile flow in the lower crust. J. Geophys. Res. 96, 4435–4456.
Lavier, L.L., Buck, W.R., Poliakov, A.N., 1999. Self-consistent rolling-hinge model for the evolution of large-offset low-angle normal faults. Geology 27, 1127–1130.
Lavier, L.L., Buck, W.R., Poliakov, A.N., 2000. Factors controlling normal fault offset in an ideal brittle layer. J. Geophys. Res. 105, 23431–23442.
Lavier, L.L., Buck, W.R., 2002. Half graben versus large-offset low-angle normal fault: importance of keeping cool during normal faulting. J. Geophys. Res. 107, ETG-8.
Lavier, L.L., Manatschal, G., 2006. A mechanism to thin the continental lithosphere at magma-poor margins. Nature 440, 324–328.
Lister, G.S., Davis, G.A., 1989. The origin of metamorphic core complexes and detachment faults formed during Tertiary continental extension in the northern Colorado River region, USA. J. Struct. Geol. 11, 65–94.
Martinez, F., Goodliffe, A.M., Taylor, B., 2001. Metamorphic core complex formation by density inversion and lower-crust extrusion. Nature 411, 930–934.
McCarthy, J., Larkin, S.P., Fuis, G.S., Simpson, R.W., Howard, K.A., 1991. Anatomy of a metamorphic core complex: seismic refraction wide-angle reflection profiling in southeastern California and western Arizona. J. Geophys. Res. 96, 12259–12291.
McGuire, A.V., 1994. Southern Basin and Range Province crust–mantle boundary: evidence from gabbroic xenoliths, Wikieup, Arizona. J. Geophys. Res. 99, 24263–24273.
McIntosh, K., Lavier, L., van Avendonk, H., Lester, R., Eakin, D., Liu, C.S., 2014. Crustal structure and inferred rifting processes in the northeast South China Sea. Mar. Pet. Geol. 58, 612–626.
McKenzie, D., Nimmo, F., Jackson, J.A., Gans, P.B., Miller, E.L., 2000. Characteristics and consequences of flow in the lower crust. J. Geophys. Res. 105, 11029–11046.
Melosh, H.J., 1990. Mechanical basis for low-angle normal faulting in the Basin and Range province. Nature 343, 331–335.
Miller, M.B., Pavlis, T.L., 2005. The Black Mountains turtlebacks: Rosetta stones of Death Valley tectonics. Earth-Sci. Rev. 73, 115–138.
Müntener, O., Hermann, J., Trommsdorff, V., 2000. Cooling history and exhumation of lower-crustal granulite and upper mantle (Malenco, Eastern Central Alps). J. Petrol. 41, 175–200.
Nagel, T.J., Buck, W.R., 2006. Channel flow and the development of parallel-dipping normal faults. J. Geophys. Res. 111, B08407.
Osmundsen, P.T., Ebbing, J., 2008. Styles of extension offshore mid-Norway and implications for mechanisms of crustal thinning at passive margins. Tectonics 27.
Poliakov, A., Cundall, P., Podladchikov, Y., Laykhovsky, V., 1993. An explicit inertial method for the simulation of viscoelastic flow: an evaluation of elastic effects on diapiric flow in two- and three-layer models. In: Stone, D.B., Runcorn, S.K. (Eds.), Flow and Creep in the Solar System: Observations, Modeling and Theory. Kluwer, Dordrecht, pp. 175–195.
Ranalli, G., 1995. Rheology of the Earth, 2nd ed. Chapman and Hall, London.
Ranero, C.R., Pérez-Gussinyé, M., 2010. Sequential faulting explains the asymmetry and extension discrepancy of conjugate margins. Nature 468, 294–299.
Regenauer-Lieb, K., Weinberg, R.F., Rosenbaum, G., 2006. The effect of energy feedbacks on continental strength. Nature 442, 67–70.
Reston, T.J., Krawczyk, C.M., Klaeschen, D., 1996. The S reflector west of Galicia (Spain): evidence from prestack depth migration for detachment faulting during continental breakup. J. Geophys. Res. 101, 8075–8091.
Rey, P.F., Teyssier, C., Whitney, D.L., 2009. Extension rates, crustal melting, and core complex dynamics. Geology 37, 391–394.
Rey, P.F., Teyssier, C., Whitney, D.L., 2010. Limit of channel flow in orogenic plateaux. Lithosphere 2 (5), 328–332.
Spencer, J.E., 1984. Role of tectonic denudation in warping and uplift of low-angle normal faults. Geology 12, 95–98.
Tan, E., Lavier, L.L., Van Avendonk, H.J.A., Heuret, A., 2012. The role of frictional strength on plate coupling at the subduction interface. Geochem. Geophys. Geosyst. 13, Q10006.
Tirel, C., Brun, J.P., Burov, E., 2008. Dynamics and structural development of metamorphic core complexes. J. Geophys. Res. 113, B04403.
Velasco, M.S., Bennett, R.A., Johnson, R.A., Hreinsdóttir, S., 2010. Subsurface fault geometries and crustal extension in the eastern Basin and Range Province, western US. Tectonophysics 488, 131–142.
Watts, A.B., 2001. Isostasy and Flexure of the Lithosphere. Cambridge University Press, Cambridge, UK.
Wernicke, B., 1981. Low-angle normal faults in the Basin and Range Province: Nappe tectonics in an extending orogen. Nature 291, 645–648.
Wernicke, B., 1985. Uniform-sense normal simple shear of the continental lithosphere. Can. J. Earth Sci. 22, 108–125.
Whitney, D.L., Teyssier, C., Rey, P., Buck, W.R., 2013. Continental and oceanic core complexes. Geol. Soc. Am. Bull. 125, 273–298.
Yin, A., 1989. Origin of regional, rooted low-angle normal faults: a mechanical model and its tectonic implications. Tectonics 8, 469–482.